Compensation mechanisms in low-temperature-grown Ga$_{1-x}$Mn$_x$As investigated by scanning tunneling spectroscopy

G. Mahieu, P. Condette, B. Grandidier, J. P. Nys, G. Allan, and D. Stiévenard
Institut d'Electronique et de Microélectronique du Nord, IEMN, (CNRS, UMR 8520) Département ISEN, 41 bd Vauban, 59046 Lille Cédex, France

Ph. Ebert
Institut für Festkörperforschung, Forschungszentrum Jülich GmbH, 52425 Jülich, Germany

H. Shimizu and M. Tanaka
Department of Electronic Engineering, The University of Tokyo, 7-3-1 Hongo, Bunkyo-ku Tokyo 113-8656, Japan

Ga$_{1-x}$Mn$_x$As layers with Mn composition of up to 6.2% are investigated by cross-sectional scanning tunneling microscopy and spectroscopy. We identify in the tunneling spectra contributions from Mn$_{Ga}^-$ acceptor states, compensating As$_{Ga}^{2+}$ donor states, and additional compensating donor states, which we suggest to be Mn$_i^{2+}$ interstitials. On basis of the observed Fermi level shift and a charge carrier compensation analysis, we deduce the concentration of Mn$_i^{2+}$ interstitials. Furthermore, scanning tunneling microscopy images suggest an inhomogeneous distribution of Mn dopant atoms. © *2003 American Institute of Physics.* [DOI: 10.1063/1.1522821]

The use of the spin of electrons in future electronic devices gained considerable interest with the discovery of diluted magnetic semiconductors, such as highly Mn-doped GaAs.[1,2] Ga$_{1-x}$Mn$_x$As becomes ferromagnetic even for low Mn concentrations[3] and is perfectly compatible with the III–V semiconductor epitaxy. In order to achieve high diluted Mn concentrations without MnAs precipitates, the Ga$_{1-x}$Mn$_x$As is commonly grown by molecular beam epitaxy (MBE) at low temperatures around 250 °C. However, at such low growth temperatures, a very high density of arsenic antisite defects (As$_{Ga}$) is incorporated due to an excess of anions. This leads to heavy compensation effects of the Mn dopants acting as shallow acceptors on Ga lattice sites in GaAs.[4] Nevertheless, with increasing Mn concentration one should expect that the material is increasingly becoming p-type, once the Mn concentration is larger than the antisite concentration (i.e., $> 1 \times 10^{20}$ cm^{-3}.)[5] However, for Mn concentrations above about 1×10^{21} cm^{-3} the Ga$_{1-x}$Mn$_x$As loses its p-type character.[3] Therefore there must be another compensation mechanism.

In order to identify this additional compensation mechanism, we investigate Ga$_{1-x}$Mn$_x$As layers with the Mn concentration x ranging from 0% to 6.2% by cross-sectional scanning tunneling microscopy (STM) and spectroscopy. We identify in the tunneling spectra contributions from Mn$_{Ga}^-$ acceptor states, As$_{Ga}^{2+}$ donor states, and additional donor states. Moreover, we observe a Fermi level shift toward p-type material with increasing Mn concentration up to about 5% Mn. Above 5% Mn, the Fermi level shifts back toward midgap. This behavior is explained by the presence of the additional donor states, which we suggest to be Mn$_i^{2+}$ interstitials. Finally, STM images show that the electronic structure fluctuates on the scale of 5 nm in the highly Mn containing material, suggesting an inhomogeneous distribution of Mn dopant atoms.

The Ga$_{1-x}$Mn$_x$As layers investigated here were grown by MBE on a (001) p^+-GaAs substrate, which was covered by a 300-nm-thick Be doped and 20-nm-thick undoped GaAs buffer layer grown both at 600 °C. The substrate temperature was then cooled down to 255 °C and a 60-nm-thick Ga$_{1-x}$Mn$_x$As layer was deposited. Different samples were grown with Mn composition x ranging from 0% to 6.2%. Finally, a 100-nm-thick GaAs cap layer was grown at 255 °C. The samples were cleaved *in situ* in ultrahigh vacuum with a base pressure $< 7 \times 10^{-9}$ Pa to expose a (110) cross-sectional surface for STM analysis. The electrochemically etched W tips were prepared in ultrahigh vacuum by annealing and self-sputtering. The spectroscopic measurements were acquired at room temperature with variable tip-sample separations as proposed by Martensson and Feenstra.[6]

Figure 1 shows typical constant-current STM images of Ga$_{1-x}$Mn$_x$As layers. The fine vertical lines are the As atomic rows in [1–10] direction. Compared to the GaAs buffer lay-
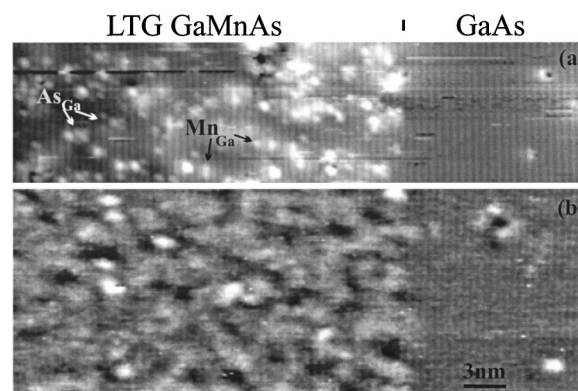

FIG. 1. STM images showing Ga$_{1-x}$Mn$_x$As layers with Mn compositions of (a) $x = 0.5\%$ and (b) $x = 6.2\%$ and the underlying buffer layer. The tunneling conditions were (a) -2.00 V and 80 pA and (b) -1.75 V and 40 pA. The gray scale ranges from 0 (black) to 2.5 Å (white).

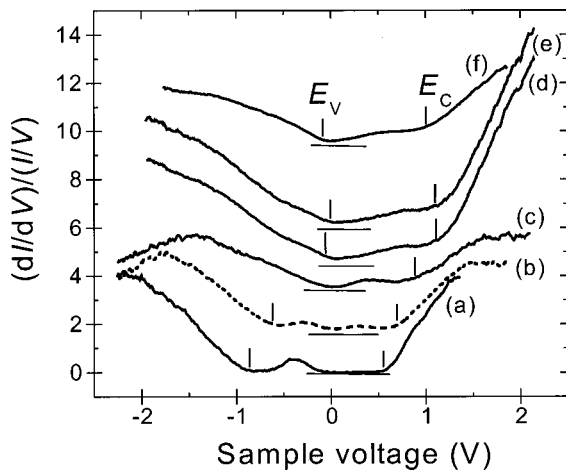FIG. 2. Tunneling spectra acquired on $Ga_{1-x}Mn_xAs$ layers for Mn compositions of (a) 0% (Ref. 5), (b) 0.5% (Ref. 5), (c) 2.8% (d) 3.2%, (e) 5.2%, and (f) 6.2%. The valence-band maximum E_V and the conduction band minimum E_C of GaAs and $Ga_{93.8}Mn_{6.2}As$ are indicated by solid lines. The horizontal lines show the zero level of each spectrum, which are shifted for clarity. The Fermi energy of each sample is located at 0 V.

FIG. 3. Calculated density of states of the valence and conduction band for $Ga_{1-x}Mn_xAs$ with different Mn concentrations. The spectra are shifted for clarity and were calculated with no compensating donors.

ers on the right-hand side, high concentrations of defects are observed in the $Ga_{1-x}Mn_xAs$ layers. These are arsenic antisite defects (marked As_{Ga}) and Mn_{Ga} dopants.[5] At high Mn compositions, the $Ga_{1-x}Mn_xAs$ layers exhibit a pronounced fluctuation of the contrast on the scale of 5 nm. This is discussed later. On the $Ga_{1-x}Mn_xAs$ layers, we acquired tunneling current–voltage $(I-V)$ spectra from which we extracted $d \ln I/d \ln V$ as a value for the density of states (Fig. 2) for the different Mn compositions. Each spectrum exhibits on the right-hand side at positive voltages and on the left-hand side at negative voltages the conduction band and valence band states, respectively. In between the spectra a band gap region is displayed, which is reduced with increasing Mn composition. In addition, we find a number of states in the band gap, depending on the Mn concentration. With no Mn [Fig. 2(a)] the low temperature-GaAs layer exhibits a pronounced band of midgap states, associated with the presence of antisite defects[7] in concentrations of 1.7×10^{20} cm^{-3} as measured in STM images.[5] A small concentration of Mn (0.5%) shifts the Fermi energy into the As_{Ga} band, splitting the defect band in an occupied and empty part, appearing as two states in the spectrum (b).[7] With further increasing Mn concentration up to 3.2%, the Fermi energy is shifted toward the valence band. Thus the As_{Ga} band is completely emptied and contributes to the density of empty states visible in the band gap [Figs. 2(c)–2(f)]. Simultaneously, the density of states (DOS) at the valence band edge changes. Additional states appear, which are associated with a band of Mn acceptors. This is corroborated by a calculation of the DOS for different Mn compositions (Fig. 3). The calculation in the tight-binding approximation simulates the perturbation potential arising from the charged Mn atoms by setting a negative unit charge on one Ga atom in a supercell. In order to keep each supercell neutral, a uniform positive background charge density was introduced. The Mn acceptor induced band overlaps completely with the GaAs valence band edge, such that the band gap is effectively reduced as visible in the calculated and measured spectra.

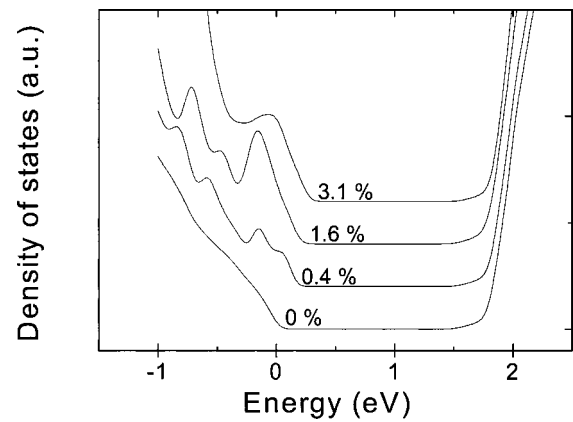The spectra in Fig. 2 show furthermore that the Fermi

level E_F shifts with the Mn composition [Fig. 4(a)]: first E_F shifts toward the valence band ($E_C - E_F$ increases) with increasing Mn concentrations of up to 5%. Above 5% Mn, E_F shifts back toward midgap. This behavior correlates well with the Mn composition dependence of the variation of the ferromagnetic transition temperature.[3] Obviously the changes in p-type character of the layers are associated with a compensation by defects. However, a single defect, such as the antisite defect, is insufficient to explain the observed shifts of Fermi energy. Indeed, with increasing Mn, the competition of Mn with the excess As for Ga lattice sites should reduce rather than increase the antisite defect concentration. Thus we need another donor state, which appears at high Mn concentrations and compensates the Mn acceptors. Because of the competition between excess As and Mn in their incorporation on Ga lattice sites, it is conceivable that at high Mn concentrations Mn is not only substitutially incorporated, but also on interstitial sites. Arsenic vacancies or Ga antisite defects cannot be expected to occur in high concentrations, because of the excess As. Ga vacancies would also be occupied by Mn or As, such that their concentrations should be negligible. Thus Mn_i interstitials are the most natural defects which could act as double donors[8] and their concentration is directly connected with the Mn concentration. The most
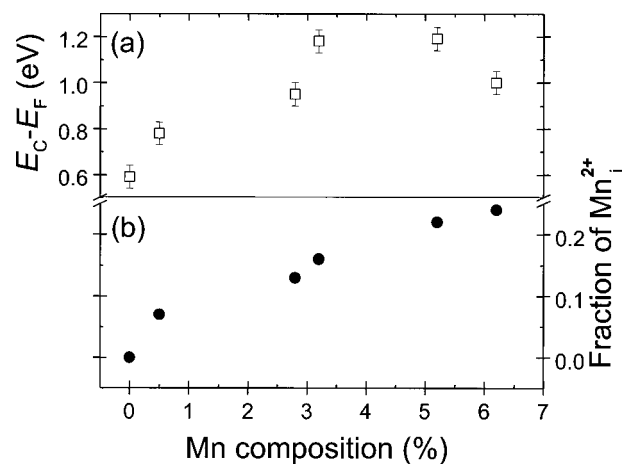

FIG. 4. (a) Shift of the Fermi level E_F relative to the conduction band edge E_C and (b) derived fraction of Mn incorporated on interstitial sites as a function of the Mn composition of the $Ga_{1-x}Mn_xAs$ layer.

probable atomic configuration is the one when a Mn atom occupies a tetrahedral interstitial position surrounded by anions.[8]

This situation can be modeled in terms of a charge balance. The charge balance n-p includes the charges induced by the single As_{Ga}^{+} antisite donor, the double As_{Ga}^{+2} antisite donor, the Mn_{Ga}^{-} acceptor, and the Mn_i^{+2} interstitial double donor. Taking the positions of the Fermi energy from the tunneling spectra [Fig. 4(a)], we calculated the occupancy probabilities for the different charge states of the antisite defects using 0.52 and 0.75 eV for the charge transfer levels $(0/+)$ and $(+/++)$, respectively, relative to E_C.[9] With this information, we extracted the fraction of Mn incorporated on interstitial sites, assuming a constant antisite defect concentration of 1.7×10^{20} cm^{-3} as measured in the STM images of the 0.5% Mn-doped layer. The resulting data in Fig. 4(b) show that the Mn_i^{+2} concentration increases up to about a quarter of all Mn in the sample. This result corroborates the expectation that with increasing Mn concentration, the concentration of the Mn_i^{+2} increases. A close look at the density of empty states in the band gap of the spectra in Figs. 2(d), and 2(e) suggests indeed a higher donor density than only that of the antisite defect [compare with Fig. 2(a)]. This is also in favor of the presence of Mn-derived donors.

At this stage we address the spatial distribution of the Mn in $Ga_{1-x}Mn_xAs$. Figure 1(b) shows that on top of the individual atomic rows, fluctuations of the apparent local density of states near the top of the valence band exist on the scale of 5 nm. As pointed out earlier the DOS at the top of the valence band is mostly due to acceptor states of Mn_{Ga}. Thus, the fluctuations of the electronic properties can be correlated with fluctuations of the Mn dopant concentration, similar to observations in Zn-doped GaAs.[10] In term of materials properties, this is a key observation in order to improve our ability to incorporate reproducibly dopant atoms with controlled concentrations and spatial distributions, as requested for nanometer scale devices.

In conclusion, cross-sectional scanning tunneling microscopy and spectroscopy of $Ga_{1-x}Mn_xAs$ layers with the Mn concentration ranging from 0% to 6.2%, was used to investigate the compensation of Mn acceptors in $Ga_{1-x}Mn_xAs$. The tunneling spectra exhibit contributions from Mn_{Ga}^{-} acceptor states, As_{Ga}^{2+} donor states, and additional donor states, which we suggest to be Mn_i^{2+} interstitials. Using the Fermi level shift behavior observed in the tunneling spectra, we extracted that the concentration of Mn_i^{2+} interstitials increases up to about one quarter of all Mn incorporated. Finally, scanning tunneling microscopy images show that the electronic structure fluctuates on the scale of 5 nm in the highly Mn containing material, suggesting an inhomogeneous distribution of Mn-dopant atoms.

[1] A. Shen, H. Ohno, F. Matsukura, Y. Sugawara, N. Akiba, T. Kuroiwa, A. Oiwa, A. Endo, S. Katsumoto, and Y. Iye, J. Cryst. Growth **175**, 1069 (1997); T. Hayashi, M. Tanaka, T. Nishimada, H. Tsuchiya, and Y. Ootuka, *ibid.* **175/176**, 1063 (1997); M. Tanaka, J. Vac. Sci. Technol. B **16**, 2267 (1998).

[2] Y. Ohno, D. K. Young, B. Beschoten, F. Matsukura, and H. Ohno, Nature (London) **402**, 790 (1999).

[3] F. Matsukura, H. Ohno, A. Shen, and Y. Sugawara, Phys. Rev. B **57**, R2037 (1998).

[4] J. M. Langer, C. Delerue, M. Lannoo, and H. Heinrich, Phys. Rev. B **38**, 7723 (1988).

[5] B. Grandidier, J. P. Nys, C. Delerue, and D. Stiévenard, Appl. Phys. Lett. **77**, 4001 (2000).

[6] P. Martensson and R. M. Feenstra, Phys. Rev. B **39**, 7744 (1988).

[7] R. M. Feenstra, J. M. Woodall, and G. D. Pettit, Phys. Rev. Lett. **71**, 1176 (1993).

[8] F. Máca and J. Mašek, Phys. Rev. B **65**, 235209 (2002).

[9] J. C. Bourgoin, H. J. von Bardeleben, and D. Stiévenard, J. Appl. Phys. **64**, R65 (1988).

[10] Ph. Ebert, T. Zhang, F. Kluge, M. Simon, Z. Zhang, and K. Urban, Phys. Rev. Lett. **83**, 757 (1999).